Desalination and Water Treatment
www.deswater.com

doi: 10.5004/dwt.2023.29321

289 (2023) 14–21
March

High-performance thin-film composite membrane consisting of a single layer of m-phenylenediamine/trimesoyl chloride fabricated via spin-assisted molecular layer-by-layer assembly

Farid Fadhillah*, Ahmad M. Alghamdi

Chemical Engineering Department, Imam Mohammad Ibn Saud Islamic University (IMSIU), Riyadh, Kingdom of Saudi Arabia, Tel.: 00966-1-125-86293, emails: fffadhillah@imamu.edu.sa (F. Fadhillah), amsalghamdi@imamu.edu.sa (A.M. Alghamdi)

Received 27 September 2022; Accepted 21 January 2023

ABSTRACT

Layer-by-layer (LbL) assembly is a versatile and robust technique for preparing ultra-thin films. The use of LbL methods for fabricating thin-film composite (TFC) polyamide (PA) membranes, termed molecular LbL (mLbL), has increased over the last decade. Here, we apply spin-assisted mLbL (SA-mLbL) assembly to fabricate a TFC PA membrane for water desalination. We selected SA-mLbL assembly because of its versatility in rapidly producing ultra-thin films with highly controlled film properties. We deposited two typical PA precursors, that is, m-phenylenediamine (MPD) and trimesoyl chloride (TMC), in an alternating fashion on a polyethersulfone ultrafiltration substrate and investigated the effects of monomer concentration and water rinsing between monomer deposition steps on membrane performance. For a feed concentration of 2,000 ppm NaCl, pressure of 34.5 bar, and temperature of 25°C, the resulting membrane achieved an NaCl rejection of 99.2% and water permeability of 0.57 $L{\cdot}m^{-2}{\cdot}h^{-1}{\cdot}bar^{-1}$ with only a single MPD/TMC layer. This result suggests that the SA-mLbL method is promising and can produce TFC PA membranes suitable for pressure-driven membrane applications.

Keywords: Molecular layer-by-layer assembly; Spin coating; Nanofiltration; Reverse osmosis; Desalination; Polyamide

1. Introduction

Over the last few decades, access to fresh water has been recognized as one of the most pervasive problems worldwide. Unfortunately, a technical note published by the Water Resources Institute indicates that this problem will worsen within the next couple of decades, such that countries that are currently considered safe will have limited access to fresh water [1]. Water desalination provides a solution to this issue, as it readily provides fresh water from seawater or saline aquifers, which account for approximately 97% of the world's total water resources.

Among desalination technologies, membrane-based desalination has increased its share in the desalination market owing to developments over the last few decades that have rendered this method competitive with thermal-based desalination techniques such as multistage flash or multi-effect distillation [2]. Reverse osmosis (RO) remains the most common technique among membrane-based desalination methods due to its mature technology. Typical RO membranes consist of a thin layer of polyamide (PA) fabricated via interfacial polymerization (IP) of m-phenylenediamine (MPD) and trimesoyl chloride (TMC) on top of a support layer, which usually consists of polysulfone and polyester webbing [3].

TMC and MPD dissolve in different solvents: TMC is typically dissolved in organic solvent while MPD is typically dissolved in water. TMC has a very low partition coefficient, which prevents its presence in an aqueous phase, while

* Corresponding author.

MPD, with its higher partition coefficient, can be present in both aqueous and organic phases. Thus, for a PA layer to form, MPD must diffuse in a water–solvent interface and immediately react with TMC [4]. One can determine the growth of a PA film from the extent of MPD diffusion in the water–solvent interface as well as the level of diffusion in the existing PA film. However, with this mechanism, it is difficult to control film properties such as thickness, morphology, or composition. Thus, the IP method usually produces relatively rough, thick PA layers.

Recently, researchers have adopted dip layer-by-layer (LbL) assembly or so-called molecular LbL (mLbL) assembly to fabricate thin layers of PA with fine-tuned layer properties, achieving control over the thickness, roughness, structure, and composition. LbL assembly is a bottom-up thin film fabrication technique based on the alternating deposition of multilayers consisting of two or more complementary materials on top of a support layer [5]. The driving force for the multilayer build-up is primarily based on electrostatic interactions, such as interactions between polyanions and polycations. However, the driving force is no longer limited to electrostatic interactions, as many other intermolecular interactions can be exploited, such as hydrogen bonding [6,7], covalent bonding [8], biological interactions [9], hydrophobic interactions [10], and coordination chemistry interactions [11]. As exemplified by conventional dip LbL assembly, the application of LbL based on coordination chemistry offers advantages over typical electrostatic interactions. By using LbL assembly based on coordination chemistry, one can precisely tune and control the chemical composition, structure, film thickness, and conformation at the atomic or molecular level. Further details about this technique can be found in an excellent review on LbL assembly written by Borges and Mano [12]. Based on LbL assembly via coordination chemistry, mLbL assembly can be applied to synthesize PA [13]. In this case, two bifunctional monomers such as MPD and TMC are assembled in an LbL fashion, as shown in Fig. 1.

MPD consists of a bifunctional group, that is, NH_2 (amine) in the form of H_2N-L-NH_2, where L is an organic fragment. TMC consists of ClOC (acyl chloride) in the form of ClOC-M-ClOCl, where M is also an organic fragment. Fig. 2 illustrates the molecular structures of MPD and TMC. The amine group of MPD and the acyl chloride group of TMC undergo a surface reaction while another amine of MPD reacts with a carbonyl (–CO) or carboxyl (–COH) functional group on a polyethersulfone (PES) support, induced by air plasma treatment [15,16]. The two steps shown in Fig. 1 can then be repeated to achieve the desired thickness.

Among the pioneers of this method for fabricating thin-film composite (TFC) membranes, Lee et al. [17,18] reported membranes with promising results. By depositing 15 layers of PA, they achieved a high NaCl rejection rate of approximately 98.7% and a permeability of 1.34 $L \cdot m^{-2} \cdot h^{-1} \cdot bar^{-1}$. The reported water flux exceeded 75% of the flux achieved by an IP-assembled PA counterpart. In addition, their mLbL PA membrane had a smoother surface than their IP-assembled PA counterpart [18,19] which is a desirable characteristic for biofouling mitigation.

Notably, in some previous works, a polyelectrolyte interlayer was deposited prior to monomer deposition. The purpose of the interlayer is to prevent the penetration of reactive monomers into the support [17,18], which can produce defects in the layer and jeopardize the membrane performance, particularly the rejection rate. Penetration within support pores is difficult to avoid and likely occurs in the case of dip mLbL because of the long duration of contact between the monomer solution and the support. With interlayer, the likelihood that penetration will occur depends on the pore size of the interlayer, yet a tighter interlayer provides an additional barrier that can reduce the water flux. Therefore, in our work, we deposited the monomers directly onto the support to avoid any additional barrier that would negatively affect the membrane flux. The penetration of monomers within the support pores is marginal in the technique used herein, that is, spin-assisted mLbL (SA-mLbL), because the very short contact time between the monomers and support layer reduces the possibility of monomer penetration into the pores.

Dip mLbL membranes have shown promising performance. However, the preparation time may present a

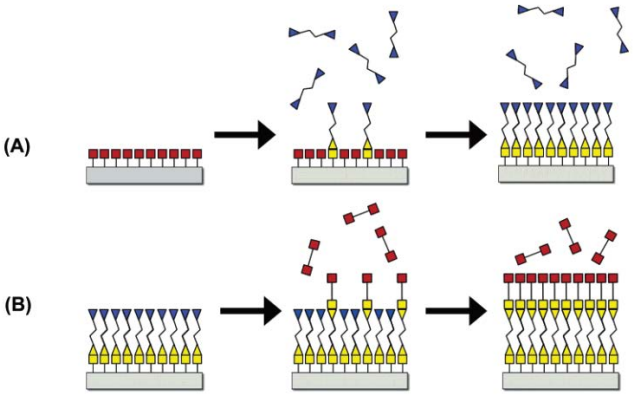

Fig. 1. Schematic of the molecular layer deposition method. (A) A-L-A bifunctional monomers react with a surface terminated with -B species (squares). (B) B-M-B bifunctional monomers react with a surface terminated with -A species (triangles). (Reprinted [adapted] with permission from the study of Du and George [14].

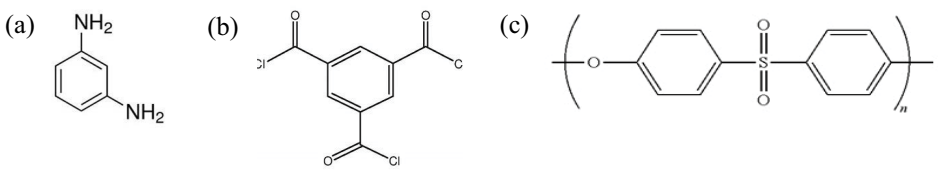

Fig. 2. Molecular structures of materials used to synthesize polyelectrolyte multilayer TFC membranes: (a) MPD, (b) TMC, and (c) PES.

drawback. The preparation of one membrane consisting of 15 MPD/TMC layers requires approximately 15 min [17,18]. This long deposition time is typical for dip LbL assembly because the monomers are allowed to naturally absorb onto the support or existing layers. To enhance the monomer adsorption, we utilized SA-mLbL assembly instead. To the best of our knowledge, SA-mLbL assembly has only recently been adopted to fabricate PA TFC membranes, as reported in 2021 by Kundu et al. [20] and Mulhearn and Stafford [21]. The latter used diaminobenzoic acid (DBA) instead of MPD.

Kundu et al. [20] reported that their membrane provided loose RO, with an NaCl rejection rate below 90% for 30 layers of PA deposited on polyvinylidene fluoride (PVDF). The authors chemically modified the PVDF using levodopa to enhance PA bonding to the support layer, that is, using levodopa-coated PVDF. Similarly, Mulhearn and Stafford reported an NaCl rejection rate slightly greater than 90% after depositing TMC/DBA layers to a thickness of approximately 20–30 nm and TMC/MPD counterparts to a thickness of 10–15 nm. This thickness corresponds to approximately 40–50 deposition cycles. Of note, both studies reported challenges in fabricating defect-free layers via SA-mLbL assembly. Therefore, a greater number of layers is needed to overcome these defects and achieve a higher rejection rate. Increasing the layer number extends the membrane preparation time and requires more reagents. In this work, we aimed to optimize the preparation conditions to fabricate defect-free LbL membranes by depositing as few layers as possible.

We successfully fabricated defect-free PA TFC membranes using SA-mLbL assembly, as confirmed by an NaCl rejection rate exceeding 98% and a reasonable permeability of approximately 0.8 $L{\cdot}m^{-2}{\cdot}h^{-1}{\cdot}bar^{-1}$. Surprisingly, these results were achieved for only a single layer of PA. These findings represent a substantial improvement for applying this method to fabricate PA RO membranes. These results suggest that the SA-mLbL method holds great potential for rapidly fabricating such membranes while maintaining high performance. The key for successful fabrication was precise control over the deposition parameters, including the concentration, spin speed, injection flow rate, and pretreatment. We investigated several fabrication protocols and assessed the effect of rinsing the deposited monomer to obtain the most suitable protocol for producing a defect-free layer. We also studied the effect of monomer concentration on membrane performance, based on our optimized protocol.

2. Materials and methods

2.1. Materials

For this work, we purchased MPD with 99% purity and TMC with 98% purity from Sigma-Aldrich (USA). For the support layer, we used TriSep UF5 ultrafiltration (UF) membranes (Sterlitech Corporation) with a pore size corresponding to a molecular weight cut-off of 5 kDa. We utilized ASTM type 1 deionized water (i.e., resistivity >18.2 MW-cm and conductivity <0.056 $mS{\cdot}cm^{-1}$) for preparing the MPD solution and for rinsing or storing the resulting membrane. Fig. 2 presents the molecular structure of the materials.

2.2. Fabrication of PA SA-mLbL membranes

For the support layer, we used a PES TriSep UF membrane pretreated in an air plasma cleaner (PDC-32-G-2, Harrick Plasma, Inc). We employed two typical monomers for PA membranes, that is, MPD and TMC. We deposited MPD and TMC in one cycle using a POLOS SPIN150i® spin coater from SPS, Inc. The spin coater was customized by the manufacturer for dispensing multiple solutions. During the deposition of MPD and TMC, the PES support was spun at a rate of 3000 rpm while the MPD and TMC solutions were injected at a rate of 0.4 $mL{\cdot}s^{-1}$ for 10 s.

As mentioned above, we investigated several protocols for fabricating a defect-free layer, which is a critical step in the application of SA-mLbL assembly. We based on investigation on three protocols as follows. In the first protocol, we performed SA-mLbL assembly with MPD and TMC deposition, without rinsing between the steps, similar to a typical IP method. This first membrane is denoted as MT. For the second protocol, we performed SA-mLbL assembly with MPD and TMC deposition, with water rinsing between the two deposition steps. This membrane is denoted as MWT. In the third protocol, we fabricated an SA-mLbL membrane from MPD and TMC with water rinsing prior to and after MPD deposition. This third membrane is denoted as WMWT. For the above investigation, we employed 2 wt.% MPD dissolved in ASTM type 1 water and 1 wt.% TMC dissolved in toluene. We used the most suitable protocol to further study the effect of monomer concentration on membrane performance, with a total of nine combinations based on 1, 1.5, and 2 wt.% MPD solution with 0.1, 0.55, and 1 wt.% TMC solution.

2.3. Permeation tests

We performed permeation tests for 5 h after each membrane equilibrated overnight under wet conditions. These tests utilized a crossflow permeation cell (Innovator® CF016, Sterlitech Corporation) with an active membrane surface area of 20.6 cm^2. The conditions for the permeation tests were as follows: pressure of 34.5 bar, feed temperature of 25°C, cross flow velocity (CFV) of 0.56 $m{\cdot}s^{-1}$, and NaCl concentration of 2000 ppm. The pH of the feed solution remained stable at approximately 6.6 without requiring any adjustments. We calculated the salt rejection rate using the following equation:

$$R = \left[1 - \frac{C_P}{C_F}\right] \times 100\% \tag{1}$$

where C_P and C_F are the concentrations of the permeate and feed in ppm, respectively. We also calculated permeability using the following equation

$$P_m = \frac{v_P}{A_m \cdot \Delta P} \tag{2}$$

where P_m is permeability in $L{\cdot}m^{-2}{\cdot}h^{-1}{\cdot}bar^{-1}$, v_p is permeate flowrate in L/h, A_m is active membrane area in m^2 and DP is operating pressure in bar.

We also examined the bare support under the same conditions and obtained a rejection rate of 18.75% ± 1.21% and a

permeability of 5.05 ± 0.33 L m^{-2} h^{-1} bar^{-1}. These values provide a benchmark for assessing the performance of the PA SA-mLbL membrane.

2.4. Film characterization

2.4.1. Hydrophilicity

We measured the membrane hydrophilicity using a Biolin Theta Flex® optical tensiometer. A 10-L water droplet was dispensed on the membrane surface at 20°C while a live-contact angle analysis of the water drop on the membrane surface was conducted for 10 s.

2.4.2. Atomic force microscopy

We utilized an atomic force microscopy (AFM) system (TOSCA from Anton Parr) in contact mode to investigate the surface morphologies of the SA-mLbL-assembled films formed on PES UF membranes. We employed silicon scanning probes with spring constants of 0.2 N/m (AP-ArrowCONTR-10 model) during the characterization process.

2.4.3. Thickness

We measured the layer thickness using a KLA Tencor AlphaStep® D-500 stylus profilometer, with a stylus speed of 0.05 mm·s^{-1} and stylus force of 0.2 mg. We acquired thickness measurements at three different locations on each sample. We coated a glass slide with a thin layer of PES and scratched the PES layer to measure its thickness. After depositing MPD/TMC on the PES-coated glass slide, we made another scratch and measure its thickness again. We then measured the MPD/TMC thickness by calculating the height difference before and after deposition.

3. Results

We successfully fabricated PA TFC membranes using SA-mLbL assembly employing TMC and MPD, with a TriSep PES UF5 membrane used as a support. A pristine PES support showed an NaCl rejection rate of 18.75% ± 1.21% and a water flux of 173.93 ± 11.46 L/h·m^2 at a pressure of 34.5 bar, temperature of 24.4°C ± 0.57°C, and NaCl concentration of 1981.5 ± 3.54 ppm. Based on this test, we considered the support to be a tight UF membrane. The membrane performance changed significantly after the deposition of the mLbL PA layer, indicating a successful deposition of MPD/TMC. In this work, we were able to fabricate a defect-free mLbL PA membrane with only a single layer, representing a significant improvement over similar works in the field, as shown in Table 1. We investigated the effect of the number of deposited MPD/TMC layers to confirm that a defect-free membrane could be attained with only a single layer, as shown in Fig. 3.

Fig. 3 shows that increasing the layer number from 1 to 2–7 did not significantly increase the rejection rate, as a relatively high rejection rate of 95% had already been obtained with only a single layer. However, the permeability decreased significantly because a thicker PA layer was formed by the

Table 1
Comparison of our mLbL PA membrane with various LbL membranes for RO applications

Membrane	Support	Method	Performance NaCl R (%), P_m (L·m^{-2}·h^{-1}·bar^{-1})	Testing condition C (ppm), P (bar), permeation cell type	References
(Polyvinylamine/poly(vinyl sulfate))$_{60}$	Polyacrylonitrile/polyethylene terephthalate	Dip	R = 98.5; P_m = 0.113	NaCl = 585; P = 40; Dead-end	[22]
(Chitosan/sodium alginate)$_{25}$	Electrospun cellulose acetate	Dip	R = 14; flux = 40 L·m^{-2}·h^{-1}	NaCl = 2,000; P = vacuum; Dead-end	[23]
PEI (PSS/PAH)	Polysulfone	Spray	R = 94; P_m = 0.75	NaCl = 2,000; P = 40; Crossflow	[24]
(PEI/PAA)–(MPD/TMC)$_{15}$	PAN	Dip	R = 98.7; P_m = 1.32	NaCl = 2,000; P = 15.5; Crossflow	[17,18]
(Naphthalene-1,3,6-trisulfonyl-chloride/piperazine)	PES	Dip	R = 95.7; P_m = 1.24	NaCl = 2,000; P = 10; Crossflow	[25]
(MPD/TMC)$_{30}$	PVDF	Spin	R = 87.3; P_m = 52.9	NaCl = 2,000; P = 34.5; Dead-end	[20]
(DBA/TMC)$_{50}$	PAN	Spin	R = 90; P_m = 2.2	NaCl = 1,000; P = 34.5; Dead-end	[21]
(MPD/TMC)$_{40}$	PAN	Spin	R = ~96; P_m = ~1.5	NaCl = 1,000; P = 34.5; Dead-end	[26]
(MPD/TMC)$_1$	PES UF	Spin	R = 99.2; P_m = 0.57	NaCl = 2,000; P = 34.5; Crossflow	This work Fig. 4 (WMWT)

PAA: polyacrylic acid; PAN: polyacrylonitrile; PAH: poly(allylamine hydrochloride); PEI: polyethylenimine; PSS: poly(sodium 4-styrenesulfonate).
C: concentration; P: pressure; Perm.: permeability; R: rejection.

higher number of layers. This result demonstrates that the membrane is defect free in the first layer.

In 2022, Krizak et al. [20] reported an SA-mLbL membrane with a permeability of 52.9 $L \cdot m^{-2} \cdot h^{-1} \cdot bar^{-1}$, which was considered extremely high and uncharacteristic for a typical RO membrane. In 2021, Mulhearn and Stafford [21] reported a more reasonable permeability–rejection relation for an RO membrane, which is comparable to our results. However, they only achieved typical RO membrane performance after 40–50 deposition cycles.

3.1. Effect of rinsing on membrane performance

In typical LbL assembly, particularly for polyelectrolyte multilayer deposition, a rinsing step is needed to stabilize weakly bound polyelectrolytes, remove unreacted molecules, and avoid contamination for deposition of a subsequent layer [12]. In contrast, the conventional IP method does not include a rinsing step after monomer deposition. As our technique is a combination of these two methods, it was imperative to determine whether a rinsing step is required. Thus, we investigated the effect of rinsing after MPD and TMC deposition.

Here, we investigated three procedures, including the MT (without water rinsing between MPD and TMC deposition), MWT (with water rinsing after MPD deposition), and WMWT (with rinsing before and after MPD deposition) protocols. As depicted in Fig. 4, rinsing played a crucial role in determining the membrane performance. In the MT membrane, the presence of excess and weakly bound MPD produced a loose layer. We also observed the presence of whitish debris in the deionized water during overnight preconditioning of the membrane prior to the permeation test. This debris may come from excess MPD and TMC that diffuse out from the resulting film and react with each other outside of the film. Thus, the loss of excess MPD and TMC after the membrane fabrication process creates voids and results in a loose film.

In contrast, for the films constructed with rinsing after MPD deposition (i.e., MWT and WMWT membranes), the excess and weakly bound monomers were washed away

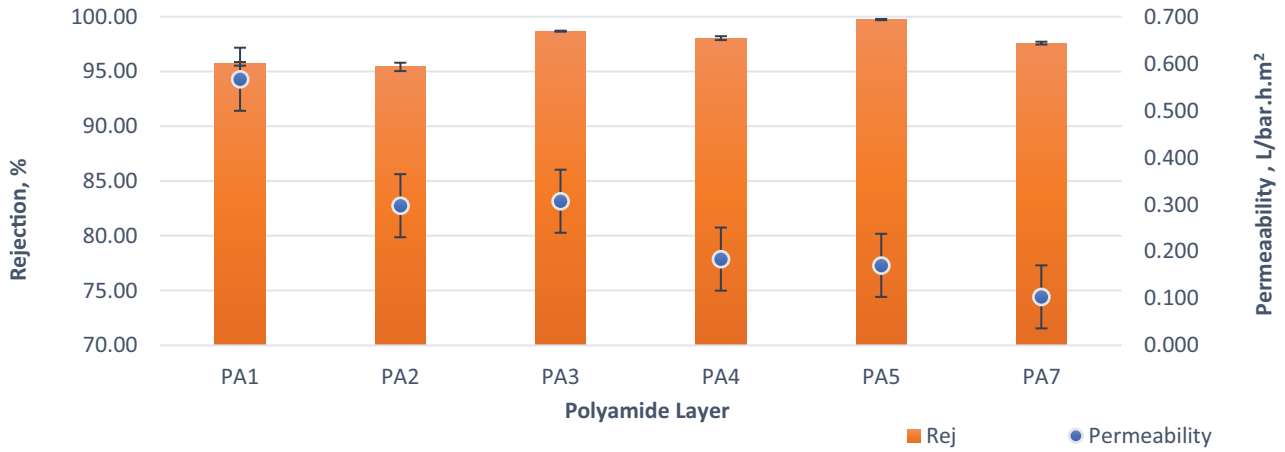

Fig. 3. Effect of the number of deposited MPD/TMC layers on membrane performance. The layers were prepared by injecting 0.2 $mL \cdot s^{-1}$ MPD and TMC for 10 s with water rinsing between MPD and TMC deposition.

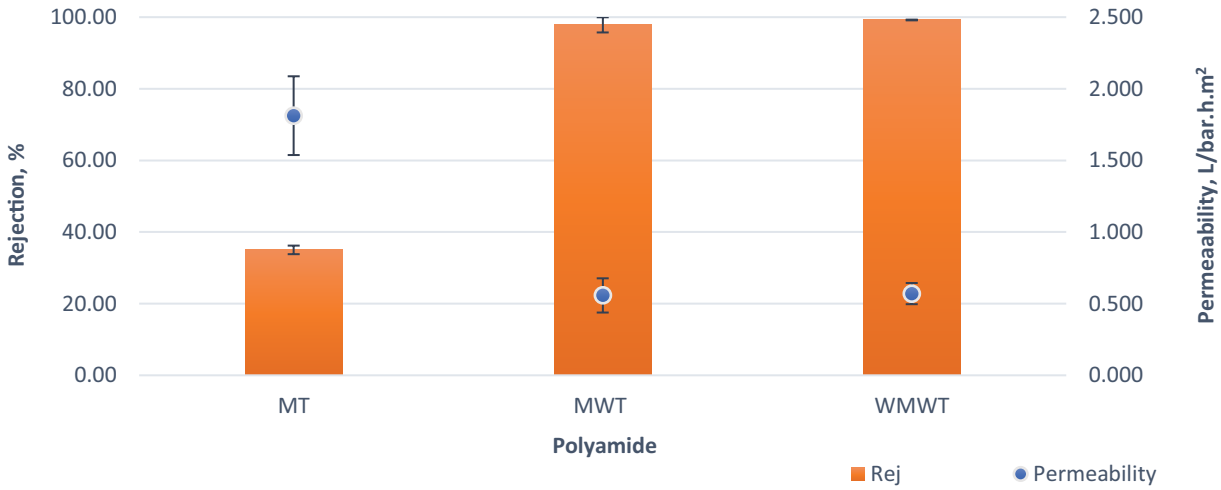

Fig. 4. Effect of water rinsing on the performance of a polyelectrolyte multilayer consisting of MPD and TMC. Testing conditions: pressure = 34.5 bar; temperature = 24.21°C ± 0.6°C; CFV = 0.56 $m \cdot s^{-1}$, NaCl concentration = 2,058.03 ± 19.10 ppm; pH = 6.57 ± 0.07.

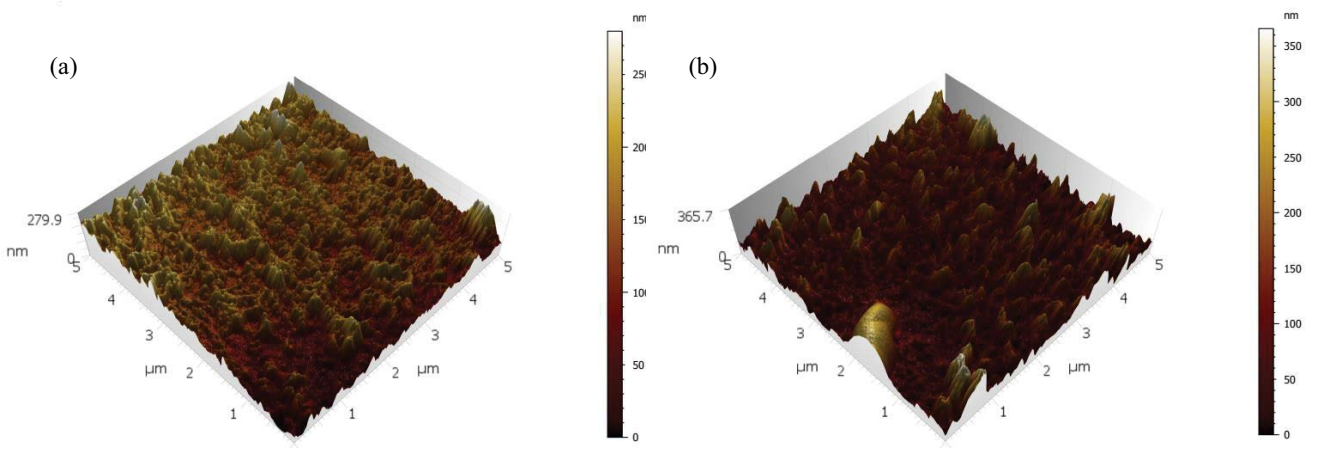

Fig. 5. AFM image of SA-mLbL PA membranes: (a) MWT and (b) MT.

prior to TMC deposition. This method resulted in a more compact film with a more entangled polymer chain, which in turn exhibited a much higher rejection rate and lower permeability.

Moreover, the surface wetting step prior to MPD deposition, that is, for the WMWT membrane, enhanced the adsorption of MPD. In this case, MPD was readily adsorbed onto the support surface owing to the compatibility between the wet surface and aqueous MPD solution. Therefore, for a given injection duration and amount of injected MPD solution, more MPD was adsorbed for the WMWT membrane than for the MWT membrane. This process thus generated a more compact film, as displayed by a higher rejection rate and lower permeability.

The rinsing step also improved the layer smoothness, as shown in Fig. 5. The MWT membrane showed a root-mean-square (RMS) roughness of 27.30 ± 4.20 nm, while the MT membrane displayed an RMS roughness of 73.04 ± 4.90 nm. This result is consistent with our surface hydrophilicity measurements. A rougher surface typically results in a higher hydrophobicity, as indicated by a greater contact angle. In this case, the smoother MWT membrane had a contact angle of 43.36° ± 0.11° while the MT membrane had a contact angle of 52.02° ± 1.29°. Importantly, the contact angle increased drastically from 21.29° ± 4.97° for the pretreated bare support to the above contact angles. The MT and MWT membranes had film thicknesses of 13.08 ± 1.67 nm and 10.32 ± 0.98 nm, respectively. All of the above measurements indicate successful coating, in addition to the change in performance between the bare support and the mLbL PA membrane.

3.2. Effect of monomer concentration

We studied the effect of monomer concentration within the range of 1–2 wt.% MPD and 0.1–1 wt.% TMC. We chose this range based on numerous previous publications that have reported concentrations within the above range. Monomer concentration plays an important role in membrane performance, as shown in Table 2. The rejection rate decreased when the membrane was prepared from a lower TMC concentration. The rejection rate was stable at a value above 96% when the TMC concentration was higher, that is, 0.55 and 1 wt.%. In contrast, for a TMC concentration of 0.1 wt.%, the rejection rate dropped below 90% and decreased further when coupled with a lower MPD concentration. For example, for an MPD concentration of 1 wt.%, the rejection rate was approximately 53% only the higher concentrations promoted the reaction and resulted in a more entangled and crosslinked layer.

Table 2
Effect of monomer concentration on permeability (P) and rejection (R)

Experiment	Concentration (wt.%)		P_m ($L \cdot m^{-2} \cdot h^{-1} \cdot bar^{-1}$)	R (%)
	MPD	TMC		
1	1	0.1	2.11 ± 0.11	53.35 ± 7.71
2	1	0.55	0.85 ± 0.10	98.36 ± 0.54
3	1	1	0.86 ± 0.01	98.86± 0.01
4	1.5	0.1	2.04 ± 0.09	67.53 ± 3.87
5	1.5	0.55	0.70 ± 0.16	97.86 ± 1.92
6	1.5	1	0.69 ± 0.01	98.85 ± 0.44
7	2	0.1	1.86 ± 0.12	84.88 ± 1.06
8	2	0.55	0.69 ± 0.01	95.37 ± 0.54
9	2	1	0.66 ± 0.10	98.65 ± 0.30

The extent of the reaction also affects the surface topology of the membrane. A more entangled and highly crosslinked layer will have a "valley and mountain" structure and a higher surface roughness. For the samples shown in Fig. 6, the roughness decreased from 27.30 ± 4.20 nm (a) to 26.56 ± 2.57 nm (b) to 21.05 ± 2.54 nm (c). Similarly, as the surface becomes smoother, the contact angle also decreases, as shown by the decrease in contact angle from 52.02° ± 1.29° (a) to 44.75° ± 0.17° (b) to 41.93° ± 1.45° (c).

4. Conclusions

In summary, we successfully fabricated TFC PA membranes utilizing SA-mLbL assembly. Our results showed that the rinsing step after monomer deposition plays an

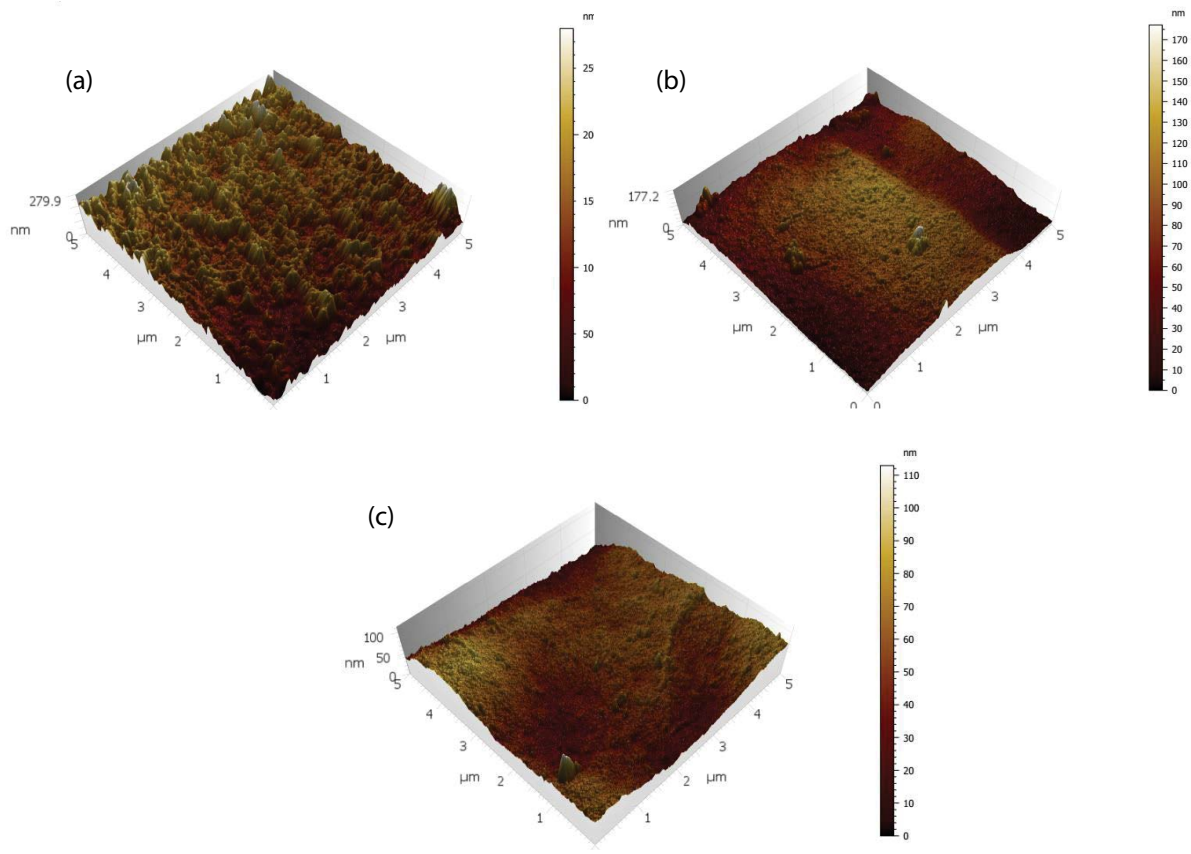

Fig. 6. AFM image of SA-mLbL MWT PA membranes prepared with (a) 2 wt.% MPD + 1 wt.% TMC, (b) 1.5 wt.% MPD + 0.55 wt.% TMC, and (c) 1 wt.% MPD + 0.1 wt.% TMC.

important role in the fabrication process. The membrane prepared without rinsing showed poor performance due to defects within the deposited PA layer. The defects were most likely caused by weakly bound monomers that were washed away during the equilibration stage and permeation testing. By controlling the preparation parameters, such as the amount of injected solution, support pretreatment, rinsing, and spin speed, we were able to fabricate high-quality TFC PA membranes using SA-mLbL assembly with only a single layer.

We also thoroughly investigated the effect of monomer concentration on membrane performance within the typical concentration range of 1–2 wt.% MPD and 0.1–1 wt.% TMC. We found that the TMC concentration significantly affects the membrane performance, including the permeability and rejection rate, while the MPD concentration had an weaker effect.

Funding

This research was funded by King Abdulaziz City of Science and Technology (KACST), grant number 14-WAT3032-08.

Acknowledgments

We thank Dr. Karim Kriaa from the Chemical Engineering Department, Imam Mohammad Ibn Saud Islamic University (IMSIU), for insightful discussions.

References

[1] T. Luo, R.S. Young, P. Reig, Aqueduct Projected Water Stress Country Rankings, World Resource Institute, 2015.
[2] L.F. Greenlee, D.F. Lawler, B.D. Freeman, B. Marrot, P. Moulin, Reverse osmosis desalination: water sources, technology, and today's challenges, Water Res., 43 (2009) 2317–2348.
[3] K.P. Lee, T.C. Arnot, D. Mattia, A review of reverse osmosis membrane materials for desalination—development to date and future potential, J. Membr. Sci., 370 (2011) 1–22.
[4] R.J. Petersen, Composite reverse osmosis and nanofiltration membranes, J. Membr. Sci., 83 (1993) 81–150.
[5] G. Decher, Fuzzy nanoassemblies: toward layered polymeric multicomposites, Science, 277 (1997) 1232–1237.
[6] B.-S. Kim, S.W. Park, P.T. Hammond, Hydrogen-bonding layer-by-layer-assembled biodegradable polymeric micelles as drug delivery vehicles from surfaces, ACS Nano, 2 (2008) 386–392.
[7] H. Lee, R. Mensire, R.E. Cohen, M.F. Rubner, Strategies for hydrogen bonding based layer-by-layer assembly of poly(vinyl alcohol) with weak polyacids, Macromolecules, 45 (2012) 347–355.
[8] J. Seo, P. Schattling, T. Lang, F. Jochum, K. Nilles, P. Theato, K. Char, Covalently bonded layer-by-layer assembly of multifunctional thin films based on activated esters, Langmuir, 26 (2010) 1830–1836.
[9] G.R. Heath, M. Li, I.L. Polignano, J.L. Richens, G. Catucci, P. O'Shea, S.J. Sadeghi, G. Gilardi, J.N. Butt, L.J.C. Jeuken, Layer-by-layer assembly of supported lipid bilayer poly-L-lysine multilayers, Biomacromolecules, 17 (2016) 324–335.
[10] M. Lorena Cortez, N. De Matteis, M. Ceolín, W. Knoll, F. Battaglini, O. Azzaroni, Hydrophobic interactions leading to a complex interplay between bioelectrocatalytic properties and multilayer meso-organization in layer-by-layer assemblies, Phys. Chem. Chem. Phys., 16 (2014) 20844–20855.

[11] F. Zhang, M.P. Srinivasan, Multilayered gold-nanoparticle/polyimide composite thin film through layer-by-layer assembly, Langmuir, 23 (2007) 10102–10108.
[12] J. Borges, J.F. Mano, Molecular interactions driving the layer-by-layer assembly of multilayers, Chem. Rev., 114 (2014) 8883–8942.
[13] P.M. Johnson, J. Yoon, J.Y. Kelly, J.A. Howarter, C.M. Stafford, Molecular layer-by-layer deposition of highly crosslinked polyamide films, J. Polym. Sci., Part B: Polym. Phys., 50 (2012) 168–173.
[14] Y. Du, S.M. George, Molecular layer deposition of Nylon 66 films examined using in situ FTIR spectroscopy, J. Phys. Chem. C, 111 (2007) 8509–8517.
[15] J. Feng, G. Wen, W. Huang, E.T. Kang, K.G. Neoh, Influence of oxygen plasma treatment on poly(ether sulphone) films, Polym. Degrad. Stab., 91 (2006) 12–20.
[16] K.S. Kim, K.H. Lee, K. Cho, C.E. Park, Surface modification of polysulfone ultrafiltration membrane by oxygen plasma treatment, J. Membr. Sci., 199 (2002) 135–145.
[17] J.-E. Gu, S. Lee, C.M. Stafford, J.S. Lee, W. Choi, B.-Y. Kim, K.-Y. Baek, E.P. Chan, J.Y. Chung, J. Bang, J.-H. Lee, Molecular layer-by-layer assembled thin-film composite membranes for water desalination, Adv. Mater., 25 (2013) 4778–4782.
[18] J.-E. Gu, J.S. Lee, S.-H. Park, I.T. Kim, E.P. Chan, Y.-N. Kwon, J.-H. Lee, Tailoring interlayer structure of molecular layer-by-layer assembled polyamide membranes for high separation performance, Appl. Surf. Sci., 356 (2015) 659–667.
[19] P.M. Johnson, J. Yoon, J.Y. Kelly, J.A. Howarter, C.M. Stafford, Molecular layer-by-layer deposition of highly crosslinked polyamide films, J. Polym. Sci., Part B: Polym. Phys., 50 (2012) 168–173.
[20] D. Krizak, M. Abbaszadeh, S. Kundu, Desalination membranes by deposition of polyamide on polyvinylidene fluoride supports using the automated layer-by-layer technique, Sep. Sci. Technol., 57 (2022) 1119–1127.
[21] W.D. Mulhearn, C.M. Stafford, Highly permeable reverse osmosis membranes via molecular layer-by-layer deposition of trimesoyl chloride and 3,5-diaminobenzoic acid, ACS Appl. Polym. Mater., 3 (2021) 116–121.
[22] W. Jin, A. Toutianoush, B. Tieke, Use of polyelectrolyte layer-by-layer assemblies as nanofiltration and reverse osmosis membranes, Langmuir, 19 (2003) 2550–2553.
[23] W. Ritcharoen, P. Supaphol, P. Pavasant, Development of polyelectrolyte multilayer-coated electrospun cellulose acetate fiber mat as composite membranes, Eur. Polym. J., 44 (2008) 3963–3968.
[24] Q. Li, G.Q. Chen, L. Liu, S.E. Kentish, Spray assisted layer-by-layer assembled one-bilayer polyelectrolyte reverse osmosis membranes, J. Membr. Sci., 564 (2018) 501–507.
[25] T. Yuan, Y. Hu, M. He, S. Zhao, H. Lan, P. Li, Q. Jason Niu, Spinning-assist layer-by-layer assembled polysulfonamide membrane for reverse osmosis from naphthalene-1,3,6-trisulfonylchloride and piperazine, J. Appl. Polym. Sci., 136 (2019) 47138, doi: 10.1002/app.47138.
[26] W.D. Mulhearn, V.P. Oleshko, C.M. Stafford, Thickness-dependent permeance of molecular layer-by-layer polyamide membranes, J. Membr. Sci., 618 (2021) 118637, doi: 10.1016/j.memsci.2020.118637.